Journal of Russian Laser Research, Volume 26, Number 5, 2005

EVANESCENT PLANE WAVES IN MULTILAYER STRUCTURES

V. S. Zuev

P. N. Lebedev Physical Institute, Russian Academy of Sciences
Leninskii Pr. 53, Moscow 119991, Russia
e-mail: zuev@sci.lebedev.ru

Abstract

We have considered evanescent plane waves in structures with a layer of a substance with $\varepsilon, \mu < 0$ and with a layer of a well-reflecting metal, $\varepsilon < 0$, $\mu \geq 1$. Waves with increased amplitude as compared with the initial wave have been found to occur, due to which evanescent waves with wave number as in the initial wave but with increased amplitude arise behind these layers. A composite material with $\varepsilon, \mu < 0$ at optical frequencies are proposed. Surface waves on a metal layer are considered in detail. It is shown that surface waves with a sufficiently arbitrary wave number can be excited. It is also shown that, on very thin layers, surface waves with wave number exceeding ten times that of a homogeneous plane wave in vacuum can be excited. Propagation losses are calculated. For a silver layer, the wave path can be from 30 up to 100 wavelengths. Practical use in developing techniques for optical transformations of short-wave surface waves in 2D space, similar to those in 3D space, are pointed out.

Keywords: nanocylinder, surface-enhanced Raman scattering, surface TM_0 wave.

1. Introduction

This work arose as a result of the work of 1967 by Veselago [1], where he pointed to the paradoxical properties of a material with simultaneously negative permeability and permittivity. It was suggested to call such a medium "left-handed" for a plane electromagnetic wave that propagates in it. In this medium and this wave, the Poynting vector $\vec{S} = (c/4\pi)\vec{E} \times \vec{H}$ has a direction opposite to the wave vector. At the interface between a traditional medium, $\varepsilon, \mu \geq 1$, and a left-handed medium, $\varepsilon, \mu < 0$, the plane wave is refracted in an exotic way, so that the wave vector of the plane refracted wave is a mirror image of the wave vector of the traditionally refracted wave, its direction being changed to the opposite. To date, artificial materials with left-handed properties in a range of microwave frequencies have been fabricated. These substances are two-dimensional sets of split rings (resonators) and wires [2]. One may think that isotropic left-handed materials would soon be developed.

A plane plate of a substance with $\varepsilon, \mu = -1$, as shown well back in [1], possesses focusing properties. The focusing properties of such a plate are stated in [3] to be perfect: it is claimed that such a lens can construct more fine structures than the wavelength of incident radiation. The same work [3] showed that for evanescent plane waves (their definition is given below) with wave number $k_x \gg (\omega/c)\sqrt{\varepsilon\mu}$ the same property is characteristic of a layer of a metal reflecting well on optical frequencies.

The work [3] triggered numerous studies whose results either disproved or confirmed the idea of the perfect lens from a left-handed material. A notion on this discussion can be formed based on the narration

Translated from a manuscript submitted August 4, 2005.
1071-2836/05/2605-0347

of it in [4, 5]. These works are also of interest *per se*, as they present quite definite, discussable arguments in favor of perfect focusing.

Arguments in favor of and against perfect focusing are developed, as a rule, by considering evanescent plane waves in an evanescent space with a left-handed medium. We shall not explore the issue of perfect focusing here, as we are not yet convinced that consideration of evanescent plane waves solves the problem of this focusing. We shall consider a more general problem, namely, the form of evanescent waves in a multilayer structure containing either a left-handed material or a well-reflecting metal. The calculations made below will show that, indeed, the amplitudes of evanescent waves both behind the layer of the substance with $\varepsilon, \mu < 0$ and behind the metal layer can (strongly) exceed the amplitude of an evanescent wave on the side facing the source. In a sense, this can serve as a proof of the idea that the focusing reproduces the near-field pattern of a vanishingly small object. In this connection, we shall discuss our proposal how to make a substance with $\varepsilon, \mu < 0$ at optical frequencies. Next, we will concentrate ourselves on evanescent waves in structures with a metal layer, on so-called surface plasmons. We will propose a method of organizing the propagation of plasmons with large amplitude and with wave number (space frequency) k_{0x} that exceeds $k_0 = \omega_0/c$, the wave number at a given frequency ω_0 in vacuum, tenfold. Propagation losses for these plasmons will be calculated. These calculations will serve as the basis for our proposal to develop the optics of highly shortened surface waves for nanooptical applications.

The evanescent wave is described by the following formulas:

$$\begin{aligned} \vec{E}(\vec{r},t) &= (E_x, E_y, E_z)e^{-\kappa_z z}e^{i(k_x x + k_y y - \omega t)}, \\ \vec{H}(\vec{r},t) &= (H_x, H_y, H_z)e^{-\kappa_z z}e^{i(k_x x + k_y y - \omega t)}. \end{aligned} \tag{1}$$

A distinction of this wave is that in the plane of constant phase the amplitude of the wave is not constant in contrast with the usual homogeneous plane wave. The wave propagates along the direction $\vec{k} = \vec{a}_x k_x + \vec{a}_y k_y$ and decays (κ_z is a real value and greater than zero) along the z axis. Note that the evanescent wave $\vec{E}(\vec{r},t) = \vec{E}e^{-\kappa_z z}e^{i(\vec{k}\vec{r}-\omega t)}$, $\vec{k} = \vec{a}_x k_x + \vec{a}_y k_y$ is not identical to the decaying wave $\vec{E}(\vec{r},t) = \vec{E}e^{-\vec{k}''\vec{r}}e^{i(\vec{k}'\vec{r}-\omega t)}$, $\vec{k} = \vec{k}' + i\vec{k}''$.

Evanescent waves occur in an experiment with total internal reflection in a medium with a smaller refraction index (see, e.g., [6]) and in experiments with the excitation of surface plasmons on a well-reflecting metal [7]. The evanescent wave is a solution of the wave equation with the characteristic equation

$$k_x^2 + k_y^2 - \kappa_z^2 = (\omega_0/c)\varepsilon\mu. \tag{2}$$

Formally, the evanescent wave (1) is a solution of the wave equation in the entire homogeneous space. However, from the physical point of view, the unlimited growth of the solution towards $z \to \infty$ is inadmissible. This means that the evanescent wave (1) is acceptable as a physical solution only in a space containing the boundary at some value of z. Exactly this situation is observed in the above mentioned experiments on the excitation of an evanescent wave.

Consider successively (i) an evanescent wave in an experiment with total internal reflection, (ii) an evanescent wave in a structure with a layer of a substance with $\varepsilon, \mu < 0$, and (iii) in a structure with a layer of a well-reflecting metal, $\varepsilon < 0$, $\mu \geq 1$.

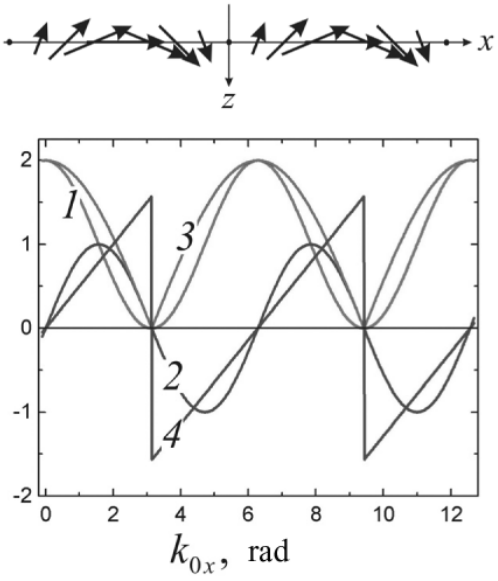

Fig. 1. Components S_{1x} (1), S_{1z} (2), modulus S_1 (3), and direction $\arctan(S_{1z}/S_{1x})$ (4) of the Poynting vector in an evanescent wave. The upper diagram shows the direction and modulus $\vec{S}$ (arrows) in the plane of the interface.

2. Evanescent Wave in an Experiment with Total Internal Reflection

The phenomenon of total internal reflection is observed when k_{0x}^2, the square of the wave number along the interface between the media, exceeds $(\omega_0/c)^2\varepsilon_1, \mu_1$. Here ε_1, μ_1 are the parameters of the medium adjacent to the total internal reflection prism with a higher refraction index. We shall consider that $k_y = 0$; the y axis, as the x axis, lies in the plane of the interface; and the z axis is directed normal to the plane of the interface towards the low-density substance. If $k_{0x}^2 > (\omega_0/c)^2\varepsilon_1, \mu_1$, then k_{2z} is a purely imaginary value. The magnitude of k_{0x}^2 increases with increase in the angle of incidence of the plane wave on the interface between the optically dense and low-density substances on the side of the dense substance. The angle of incidence is reckoned from the normal to the interface. The limiting large value of k_{0x}^2 is equal to $(\omega_0/c)^2\varepsilon, \mu$. Here ε, μ are the parameters of the material of the prism. In the medium with ε_1, μ_1, there occurs an evanescent wave propagating along x on the interface and vanishing along z, i.e., along the normal to the surface.

It would be useful to see here how the Poynting vector behaves in an evanescent wave. The data of the calculations are given in Fig. 1. The lower fragment of the figure shows the tangential and normal components S_{1x}, S_{1z} of the Poynting vector, its modulus S_1 and direction $\arctan(S_{1z}/S_{1x})$ relative to the plane of the interface. In the upper fragment, the arrows show the direction and modulus of $\vec{S}_1$ in the plane of the interface. In the evanescent wave, on average, there is no energy flux along the z axis, along the normal to the interface. Along the x axis, there is a directed energy flux. In the known experiment with the so-called disturbed total internal reflection, though, the evanescent wave passes the energy along the z axis. A respective device is used in laser experiments.

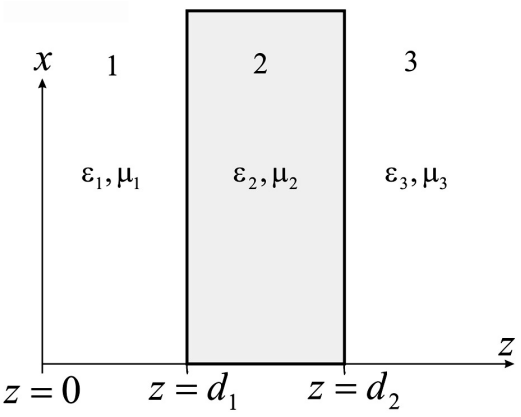

Fig. 2. Three-layer structure, designations.

3. Inhomogenous Wave in a Structure with a Layer of a Substance with $\varepsilon, \mu < 0$

We shall consider a structure consisting of three plane layers of a substance, see Fig. 2. Layers 1 and 3 shall be considered substances with the traditional properties, $\varepsilon_1, \mu_1 \geq 1$ and $\varepsilon_3, \mu_3 \geq 1$; layer 2, a left-handed substance with $\varepsilon_2, \mu_2 < 0$. In region 1, there is an evanescent wave

$$\begin{aligned} H_{0y}(\vec{r},t) &= H_{0y}e^{-\kappa_{0z}z}e^{i(k_{0x}x-\omega t)}, \\ E_{0x}(\vec{r},t) &= i\frac{c\kappa_{0z}}{\omega\varepsilon_1}H_{0y}e^{-\kappa_{1z}z}e^{i(k_{0x}x-\omega t)}, \\ E_{0z}(\vec{r},t) &= -\frac{ck_{0x}}{\omega\varepsilon_1}H_{0y}e^{-\kappa_{0z}z}e^{i(k_{0x}x-\omega t)}. \end{aligned} \tag{3}$$

In the wave, we choose the subscript 0 as in the incident wave, though, certainly, it is not incident on the interface at $z = d_1$ as it moves along x, but is adjacent to this interface and penetrates it. As in [3], we shall consider that $\varepsilon_1/\mu_1 = \varepsilon_2/\mu_2 = \varepsilon_3/\mu_3$ and there is no reflection and, therefore, is no need to introduce reflected waves into consideration. The wave to the right of the interface $z = d_1$ (the wave index $i = 2$) shall be sought for as

$$\begin{aligned} H_{iy}(\vec{r},t) &= H_{iy}e^{ik_{iz}z}e^{i(k_{ix}x-\omega t)}, \\ E_{ix}(\vec{r},t) &= \frac{ck_{iz}}{\omega\varepsilon_j}H_{iy}e^{ik_{iz}z}e^{i(k_{ix}x-\omega t)}, \\ E_{iz}(\vec{r},t) &= -\frac{ck_{ix}}{\omega\varepsilon_j}H_{iy}e^{ik_{iz}z}e^{i(k_{ix}x-\omega t)}. \end{aligned} \tag{4}$$

The electric field components $E_{ix}(\vec{r},t)$ and $E_{iz}(\vec{r},t)$ follow from the expression for $H_{iy}(\vec{r},t)$ by the equation $\mathrm{rot}\vec{H} = (\varepsilon/c)(\partial\vec{E}/\partial t)$. The amplitude of this wave shall be determined, using the boundary conditions

$$\begin{aligned} H_{0y}(\vec{r},t)|_{z=d_1} + H_{1y}(\vec{r},t)|_{z=d_1} &= H_{2y}(\vec{r},t)|_{z=d_1}, \\ E_{0x}(\vec{r},t)|_{z=d_1} + E_{1x}(\vec{r},t)|_{z=d_1} &= E_{2x}(\vec{r},t)|_{z=d_1}. \end{aligned} \tag{5}$$

In this case, $H_{1y}(\vec{r},t)|_{z=d_1} = 0$ and $E_{1x}(\vec{r},t)|_{z=d_1} = 0$, as there is no reflected wave. The result is as follows:

$$\begin{aligned} k_{2x} = k_{0x}, \qquad k_{2z} = -i\kappa_{0z}\frac{e_2}{\varepsilon_1}, \qquad e_2 = \varepsilon_2, \\ H_{2y}(\vec{r},t) &= H_{0y}e^{-\kappa_{0z}d_1(1+e_2/\varepsilon_1)}e^{\kappa_{0z}(e_2/\varepsilon_1)z}e^{i(k_{0x}x-\omega t)}, \\ E_{2x}(\vec{r},t) &= i\frac{c\kappa_{0z}}{\omega\varepsilon_1}H_{0y}e^{-\kappa_{0z}d_1(1+e_2/\varepsilon_1)}e^{\kappa_{02}(e_2/\varepsilon_1)z}e^{i(k_{0x}x-\omega t)}, \\ E_{2z}(\vec{r},t) &= \frac{ck_{0x}}{\omega e_2}H_{0y}e^{-\kappa_{0z}d_1(1+e_2/\varepsilon_1)}e^{\kappa_{0z}(e_2/\varepsilon_1)z}e^{i(k_{0x}x-\omega t)}. \end{aligned} \tag{6}$$

From (6), it is seen that the evanescent wave behaves paradoxically in a layer of a substance with $\varepsilon_2, \mu_2 < 0$. The wave grows along the coordinate z. Note that, when deducing (6), we did not have to choose the sign in k_{2z}. The sign of k_{2z} was determined from the equations.

There is no need for special calculation of the Poynting vector on the left- and right-hand side from the interface, $z = d_1$. Its normal components on the left and on the right shall be equal to one another. But $\vec{S}_n = \vec{a}_z(c/4\pi)E_xH_y$, i.e., is equal to the product of the tangential components of the field, E_x and H_y. Since, when applying the boundary conditions, we equated these components, it is clear without calculations that the equality $\vec{S}_{0n}\Big|_{z=d_1} = \vec{S}_{2n}\Big|_{z=d_1}$ holds.

Let us now consider the field at the interface $z = d_2$, see Fig. 2. We will need the formulas for the "incident" and transmitted waves, and the reflected wave is absent as we chose $\varepsilon_2/\mu_2 = \varepsilon_3/mu_3$. In this case, the "incident" wave is described by formulas (6), and the transmitted wave shall again be sought as (4). The boundary conditions are described by formulas (5), in which the subscript 0 should be replaced by 2, 2 by 3, and d_1 by d_2. The result is as follows:

$$\begin{aligned} k_{3x} = k_{0x}, \qquad k_{3z} = i\kappa_{0z}\frac{\varepsilon_3}{\varepsilon_1}, \\ H_{3y}(\vec{r},t) &= H_{0y}e^{-\kappa_{0z}d_1(1+e_2/\varepsilon_1)}e^{\kappa_{0z}d_2(e_2/\varepsilon_1+\varepsilon_3/\varepsilon_1)}e^{\kappa_{0z}(e_2/\varepsilon_1)z}e^{i(k_{0x}x-\omega t)}, \end{aligned} \tag{7}$$

Figure 3 shows the distribution of the field along the z axis in a homogeneous space and in a space with a layer of a substance with $\varepsilon_2, \mu_2 < 0$ located between $z = d_1$ and $z = d_2$. The evanescent wave decays exponentially in the regions $0 \le z \le d_1$ and $d_2 \le z$ and grows exponentially in the region $d_1 \le z \le d_2$. The field of the evanescent wave H_{3y}, penetrating over the layer of the substance with $\varepsilon_2, \mu_2 < 0$, again becomes equal to the initial (in the plane $z = 0$) value H_{0y} in the plane

$$z_0 = d_2(e_2 + \varepsilon_3)/\varepsilon_3 - d_1(e_2 + \varepsilon_1)/\varepsilon_3. \tag{8}$$

This plane is the same for all κ_{0x}.

Formulas (6) contain no explicit dependence on μ_1, μ_2, μ_3. This dependence is contained implicitly in κ_{0z} and k_{0x}. At $k_{0x} \gg (\omega/c)\sqrt{\varepsilon_1\mu_1}$, when the equality $\kappa_{0z} \approx \kappa_{2z}$ holds approximately, this explicit dependence can be neglected. But the negative sign in μ_2 at negative ε_2 enabled us to admit the absence of reflected waves. At positive μ_2, reflected waves inevitably occur.

The observed independence on μ_2 served in [3] as a reason for considering the evanescent wave in a space with a layer of a substance with $\varepsilon_2 < 0$, $\mu_2 \ge 1$. These properties are characteristic of well-reflecting metals at optical frequencies. The work [3] demonstrated in electrostatic approximation for Maxwell equations the effect of approximated preservation of the subwave structure of the field behind a small-thickness metal layer. We shall make here a similar consideration, using the above method of eigenwaves and boundary conditions.

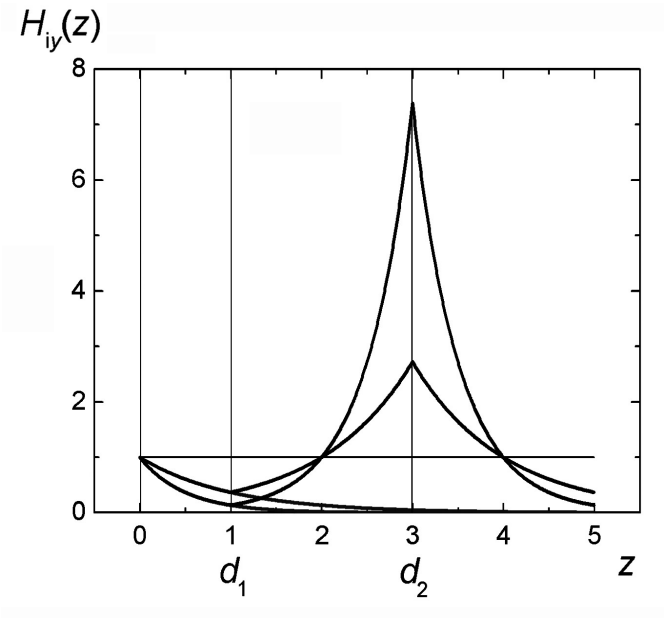

Fig. 3. Distribution of the field in an evanescent wave in a structure with a layer of a substance $\varepsilon_2, \mu_2 < 0$. Two waves for two values of κ_{0x} are shown.

4. Evanescent Wave in a Space with a Layer of Well-Reflecting Metal

We shall again consider a structure consisting of three plane layers of a substance, see Fig. 2. Layers 1 and 3 shall be considered substances with $\varepsilon_1, \mu_1 \geq 1$ and $\varepsilon_3, \mu_3 \geq 1$; layer 2, a well-reflecting metal, $\varepsilon_2 < 0, \mu_2 \geq 1$. In region 1, there is an evanescent wave, with wave index $i = 0$, which in this case has the form of (3). Besides an incident wave in layer 1, there is a reflected wave, with wave index $i = 1$, since $\varepsilon_1/\mu_1 \neq \varepsilon_2/\mu_2$. The reflected wave is described by formulas of the form (4) upon substitution of the subscripts i and j by 1. We shall assume that the reflected wave has no effect on the source of the incident wave, as it decays exponentially towards negative z, as will be clear later, and its repeated reflections can be neglected. In layer 2, which we consider yet infinitely extended, there is a transmitted wave that is described by formulas (4) with subscripts $i = 2$, $j = 2$. Again, we apply the boundary conditions and, as a result, obtain ($e_2 = -\varepsilon_2$):

$$k_0 x = k_1 x = k_2 x, \tag{9}$$

$$H_{1y}(\vec{r}, t) = \frac{1 + \kappa_{2z}\varepsilon_1/\kappa_{0z}e_2}{1 - \kappa_{2z}\varepsilon_1/\kappa_{0z}e_2} H_{0y} e^{\kappa_{0z}(z-d_1)} e^{i(k_{0x}x - \omega t)}, \tag{10}$$

$$H_{2y}(\vec{r}, t) = \frac{2}{1 - \kappa_{2z}\varepsilon_1/\kappa_{0z}e_2} H_{0y} e^{-\kappa_{2z}(z-d_1)} e^{i(k_{0x}x - \omega t)}. \tag{11}$$

At $\kappa_{2z}\varepsilon_1/\kappa_{0z}e_2 = 1$, the amplitudes of the reflected and transmitted waves become infinitely large. This infinitely disappears when we take into account the losses in medium 2. The phenomenon of resonance is observed. If we calculate k_{0x} taking into account the latter equality $\kappa_{2z}\varepsilon_1/\kappa_{0z}e_2 = 1$, we obtain

$$k_{0x}^2 = (\omega/c)^2 \varepsilon_1 \varepsilon_2 \frac{\varepsilon_1\mu_2 - \varepsilon_2\mu_1}{(\varepsilon_- \varepsilon_2)(\varepsilon_1 + \varepsilon_2)}. \tag{12}$$

At $\mu_1 = \mu_2 = 1$ we obtain a well-known formula $k_{0x}^{\rm pl} = (\omega/c)\sqrt{\varepsilon_1\varepsilon_2/(\varepsilon_1+\varepsilon_2)}$ for the wave number of the surface plasmon; see, e.g., [7]. Thus, formulas (10) and (11) demonstrate the existence of surface-plasmon resonance.

Now we consider the evanenscent wave in a space with a plane metal layer of restricted extent along z. As previously, we will mean a well-reflecting metal, $\varepsilon_2 < 0$, $\mu_2 \geq 1$. The space structure and designations are the same as in Fig. 2. In this case, one needs to consider an incident wave with subscript 0, a wave reflected by the interface at $z = d_1$ with subscript 1, a wave that penetrated the metal layer with subscript 2, a wave reflected at the interface $z = d_2$ with subscript r, and a wave that penetrated space 3 with subscript 3. There are grounds to believe that

$$k_{0z} = i\kappa_{0z}, \qquad k_{1z} = i\kappa_{0z}, \qquad k_{2z} = i\kappa_{2z}, \qquad k_{rz} = -i\kappa_{2z}, \qquad k_{3z} = i\kappa_{0z}. \tag{13}$$

Herewith, we assume that $\varepsilon_3 = \varepsilon_1$. The waves are chosen as follows:

	$k_{0z} = i\kappa_{0z},$
$H_{iy}(\vec{r}) = H_{iy}e^{ik_{iz}z},$	$H_{0y}(\vec{r}) = H_{0y}e^{-\kappa_{0z}z},$
$E_{ix}(\vec{r}) = (ck_{iz}/\omega\varepsilon_j)H_{iy}e^{k_{iz}z},$	$E_{0x}(\vec{r}) = i(c\kappa_{0z}/\omega\varepsilon_1)H_{0y}e^{-\kappa_{0z}z},$
$E_{iz}(\vec{r}) = -(ck_{ix}/\omega\varepsilon_j)H_{iy}e^{k_{iz}z},$	$E_{0z}(\vec{r}) = -(ck_{0x}/\omega\varepsilon_1)H_{0y}e^{-\kappa_{0z}z},$
$k_{1z} = -i\kappa_{0z},$	$k_{2z} = i\kappa_{2z},$
$H_{1y}(\vec{r}) = H_{1y}e^{\kappa_{0z}z},$	$H_{2y}(\vec{r}) = H_{2y}e^{-\kappa_{2z}z},$
$E_{1x}(\vec{r}) = -i(c\kappa_{0z}/\omega\varepsilon_1)H_{1y}e^{\kappa_{0z}z},$	$E_{2x}(\vec{r}) = -i(c\kappa_{2z}/\omega e_2)H_{2y}e^{-\kappa_{2z}z},$
$E_{1z}(\vec{r}) = -(ck_{0x}/\omega\varepsilon_1)H_{1y}e^{\kappa_{0z}z},$	$E_{2z}(\vec{r}) = (ck_{0x}/\omega e_2)H_{2y}e^{-\kappa_{2z}z},$
$k_{rz} = -i\kappa_{2z},$	$k_{3z} = i\kappa_{0z},$
$H_{ry}(\vec{r}) = H_{ry}e^{\kappa_{2z}z},$	$H_{3y}(\vec{r}) = H_{3y}e^{-\kappa_{0z}z},$
$E_{rx}(\vec{r}) = i(c\kappa_{2z}/\omega e_2)H_{ry}e^{\kappa_{2z}z},$	$E_{3x}(\vec{r}) = i(c\kappa_{0z}/\omega\varepsilon_1)H_{3y}e^{-\kappa_{0z}z},$
$E_{rz}(\vec{r}) = (ck_{0x}/\omega e_2)H_{ry}e^{\kappa_{2z}z},$	$E_{3z}(\vec{r}) = -(ck_{0x}/\omega\varepsilon_1)H_{3y}e^{-\kappa_{0z}z}.$

We will use the boundary conditions at the interfaces.

Field on the left from $z = d_1$	Field on the right from $z = d_1$
$H_{sy}^{d_1\varepsilon_1}\big\vert_{z=d_1} = H_{0y}e^{-\kappa_{0z}d_1} + H_{1y}e^{\kappa_{0z}d_1},$	$H_{sy}^{d_1\varepsilon_2}\big\vert_{z=d_1} = H_{2y}e^{-ik_{2z}d_1} + H_{ry}e^{ik_{rz}d_1},$
$E_{sx}^{d_1\varepsilon_1}\big\vert_{z=d_1} = i\frac{c\kappa_{0z}}{\omega\varepsilon_1}\left(H_{0y}e^{-\kappa_{0z}d_1} - H_{1y}e^{\kappa_{0z}d_1}\right),$	$E_{sx}^{d_1\varepsilon_2}\big\vert_{z=d_1} = \frac{c}{\omega\varepsilon_2}\left(k_{2z}H_{2y}e^{ik_{2z}d_1} + k_{rz}H_{ry}e^{ik_{rz}d_1}\right),$

Field on the left from $z = d_2$	Field on the right from $z = d_2$
$H_{sy}^{d_2\varepsilon_2}\big\vert_{z=d_2} = H_{2y}e^{ik_{2z}d_2} + H_{ry}e^{ik_{rz}d_2},$	$H_{3y}^{d_2\varepsilon_2}\Big\vert_{z=d_2} = H_{3y}e^{ik_{3z}d_2},$
$E_{sx}^{d_2\varepsilon_2}\big\vert_{z=d_2} = \frac{c}{\omega}\left(\frac{k_{rz}}{\varepsilon_2}H_{ry}e^{ik_{rz}d_2} + \frac{k_{2z}}{\varepsilon_2}H_{2y}e^{ik_{2z}d_2}\right),$	$E_{sx}^{d_2\varepsilon_2}\big\vert_{z=d_2} = \frac{ck_{3z}}{\omega\varepsilon_3}H_{3y}e^{ik_{3z}d_2},$

As a result, we have the following equations:

$$\begin{aligned}
H_{1y} - H_{2y} + 0\cdot H_{3y} - H_{ry} &= -H_{0y},\\
-H_{1y} + \frac{\kappa_{2z}\varepsilon_1}{\kappa_{0z}e_2}H_{2y} + 0\cdot H_{3y} - \frac{\kappa_{2z}\varepsilon_1}{\kappa_{0z}e_2}H_{ry} &= -H_{0y},\\
0\cdot H_{1y} + H_{2y}e^{-(\kappa_{2z}-\kappa_{0z})d_2} - H_{3y} + H_{ry}e^{(\kappa_{2z}+\kappa_{0z})d_2} &= 0,\\
0\cdot H_{1y} - \frac{\kappa_{2z}\varepsilon_1}{\kappa_{0z}e_2}H_{2y}e^{-(\kappa_{2z}-\kappa_{0z})d_2} - H_{3y} + \frac{\kappa_{2z}\varepsilon_1}{\kappa_{0z}e_2}H_{ry}e^{(\kappa_{2z}+\kappa_{0z})d_2} &= 0.
\end{aligned} \tag{14}$$

The determinant of this system of linear equations has the following form:

$$\Delta = \begin{vmatrix} 1 & -1 & 0 & -1\\ -1 & K & 0 & -K\\ 0 & e1 & -1 & e2\\ 0 & -Ke1 & -1 & Ke2 \end{vmatrix} = -(K-1)^2 e2 + (K+1)^2 e1, \tag{15}$$

$$e1 = e^{-(\kappa_{2z}-\kappa_{0z})d_2}, \qquad e2 = e^{(\kappa_{2z}+\kappa_{0z})d_2}, \qquad K = \kappa_{2z}\varepsilon_1/\kappa_{0z}e_2.$$

The calculations yield the following result:

$$\begin{aligned}
H_{1y} &= -H_{0y}\frac{(K-1)(K+1)(1-e1/e2)}{(K-1)^2-(K+1)^2 e1/e2},\\
H_{2y} &= -2H_{0y}\frac{(K-1)}{(K-1)^2-(K+1)^2 e1/e2},\\
H_{3y} &= -4H_{0y}\frac{Ke1}{(K-1)^2-(K+1)^2 e1/e2},\\
H_{ry} &= -2H_{0y}\frac{(K+1)e1/e2}{(K-1)^2-(K+1)^2 e1/e2}.
\end{aligned} \tag{16}$$

There is the plasmon resonance at two values of K:

$$K = \frac{\kappa_{2z}\varepsilon_1}{\kappa_{0z}e_2} = \begin{cases} \frac{1+\sqrt{e1/e2}}{1-\sqrt{e1/e2}} &= \frac{1+e^{-\kappa_{2z}d_2}}{1-e^{-\kappa_{2z}d_2}},\\ \frac{1-\sqrt{e1/e2}}{1+\sqrt{e1/e2}} &= \frac{1-e^{-\kappa_{2z}d_2}}{1+e^{-\kappa_{2z}d_2}}. \end{cases} \tag{17}$$

The effect of the splitting of the surface-plasmon resonance in a limited-thickness metal layer was discussed in detail in [8]. The splitting is due to the existence of the symmetric and antisymmetric modes. Note, by the way, that in a metal cylinder the splitting for the plasmon mode TM_0 is absent owing to complete axial symmetry. At a small thickness of the metal layer, the splitting of the resonance is large, as $1 + e^{-\kappa_{2z}d_2} \gg 1 - e^{-\kappa_{2z}d_2}$, and at a large thickness of the layer, when $e^{-\kappa_{2z}d_2} \ll 1$, the splitting is small, and the resonance value of K is approximately 1, which coincides with the earlier obtained value for a metal layer of unrestricted thickness.

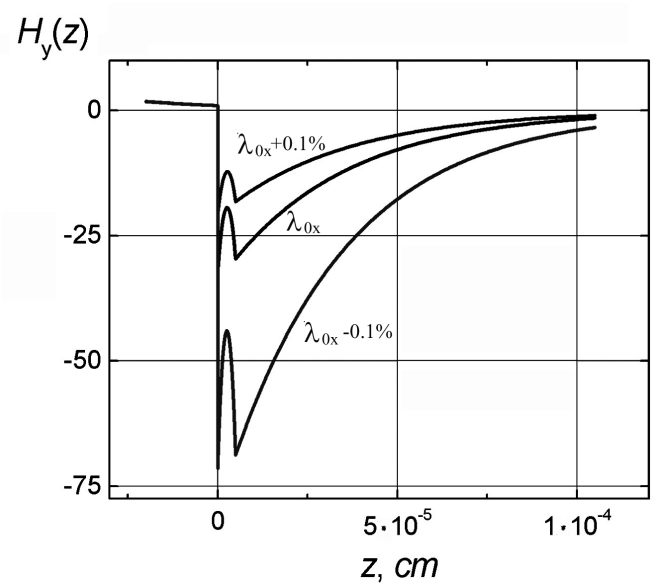

Fig. 4. An evanescent wave in a space with a silver layer for $\kappa_{0x} + 0\%, \pm 0.1\%$. $H_{0y}(z = 0) = 1$. Ag at $0 < z < 50$ nm.

Let us construct the fields, see Fig. 4. For silver, $\varepsilon_2 = -10.67$ and $\mu_2 = 1$ at a wavelength $\lambda_0 = 514.7$ nm [9].

$$
\begin{array}{lcll}
H_y(\vec{r},t) & = & H_{0y}e^{-\kappa_{0z}z}, & -d_1 < z \le 0, \\
H_y(\vec{r},t) & = & H_{2y}(\vec{r},t) + H_{ry}(\vec{r},t) & \\
 & = & -2H_{0y}\frac{(K-1)e^{-\kappa_{2z}z}+(K+1)e^{-2\kappa_{2z}d_2}e^{\kappa_{2z}z}}{(K-1)^2-(K+1)^2e^{-2\kappa_{2z}d_2}}, & 0 < z \le d_2, \\
H_y(\vec{r},t) & = & H_{3y}e^{-\kappa_{0z}z} & \\
 & = & -4H_{0y}\frac{Ke^{-(\kappa_{2z}z-\kappa_{0z})d_2}e^{-\kappa_{0z}z}}{(K-1)^2-(K+1)^2e^{-2\kappa_{2z}d_2}}, & d_2 < z.
\end{array}
$$

Unlike the case with a layer of a substance with $\varepsilon, \mu < 0$, here we observe a significant dispersion, the dependence of the effect of the amplification of the field by the adjacent layer of the substance on κ_{0x}. The structure of the field is also completely different.

The results of considering the evanescent plane wave in a layer structure are the plots in Figs. 3 and 4. Behind the layer of a substance with $\varepsilon = -1$, $\mu = -1$, as well as behind the layer of a well-reflecting metal, $\varepsilon < 0$, $\mu = 1$, the amplitude of the evanescent wave proves to be significantly increased as compared with its value on the side of the layer facing the source. The effect in the structure with the layer $\varepsilon = -1$, $\mu = -1$ has no dependence on the wave number k_{0x} of the evanescent wave (has no dispersion), and in the structure with the metal layer the dispersion of the effect is great. Despite some similarity of the final result, the form of the fields in the two layers considered has different dependences on the transverse coordinate.

The rise in amplitude of the evanescent wave in the transverse direction does not violate the energy conservation law. The fact is that the above problems are not problems for the propagation of electromagnetic radiation, but are meant to search for the eigenwaves $\vec{H}_n(\vec{r})$ of the time-free wave equation

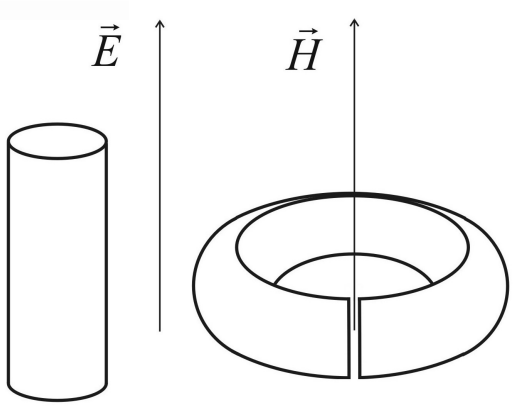

Fig. 5. A nanocylinder and a nanoring as half-wave resonators for surface plasmons: the core is an electric dipole resonator; the ring, a magnetic dipole resonator. The ring is shown enlarged three times as compared with the core.

$\Delta\vec{H}(\vec{r}) + (\omega/c)^2\varepsilon\mu\vec{H}(\vec{r}) = 0$ in an evanescent space, i.e., with respective boundary conditions. The problem for propagation is the search for the solution of equation $\Delta\vec{H}(\vec{r},t) - (1/\nu)\vec{H}(\vec{r},t) = 0$ in the form $\vec{H} = \sum\limits_n \left[a_n(t)\vec{H}_n + a_n^*(t)\vec{H}_n^*\right]$, where $\vec{H}_n(\vec{r})$ are the solutions of the time-free wave equation. The problem is beyond the scope of this consideration.

The field in the space with a metal layer affected by the evanescent wave contains simultaneously five evanescent waves. These are the acting wave H_{0y}, the wave H_{1y} reflected from the first interface, the wave H_{2y} that penetrates the metal layer, the wave H_{ry} reflected by the second interface, and the wave H_{3y} that penetrates over the metal layer. For definiteness, we chose for the discussion the transverse magnetic wave H_{iy}, i.e., a TM wave. The amplitudes of the waves H_{1y}, H_{2y}, H_{ry}, and H_{3y} significantly exceed that of H_{oy}. Under conditions of surface-plasmon resonance, these amplitudes turn to infinity (in the absence of the losses), whereas H_{0y} remains finite. The boundary condition of the equality of the tangential components of the fields at the first interface is met due to the approximate equality of H_{1y} and H_{2y} at this interface. At the second interface, the effect is repeated: the wave H_{2y}, being small at the second interface, generates the waves H_{ry} and H_{2y}, approximately equal and larger in amplitude. The waves H_{1y}, H_{2y} and H_{ry}, H_{3y}, acting pairwise, form surface waves at the first and second interface of the metal, respectively.

5. Surface Plasmons on Metal Wires and Thin Netal Layers

We shall not discuss further the evanescent waves in a medium with $\varepsilon = -1$, $\mu = -1$. At the moment, a topical problem is the search for or fabrication of a material with $\varepsilon = -1$, $\mu = -1$ at optical frequencies. Possibly, such materials can be composites from metal rods and the same rods bent into split rings, see Fig. 5. Each of these elements supports a surface plasmon and is in one instance an electric dipole resonator excited by an electric field $\vec{E}$ of an incident wave and in the other instance a magnetic dipole resonator excited by the magnetic field $\vec{H}$ of the incident wave. Just the surface plasmons on rods and rings are what distinguishes our proposal from that presented in [2]. The wavelength of the surface plasmon on a small-diameter cylinder is tens of times smaller than that in a free space [10]. The structural

elements shaped as rods and rings and possessing a half-wave resonance will be small as compared with the wavelength in a free space. At frequencies near the resonance frequency the composite medium will have $\varepsilon < 0$, $\mu < 0$ and will not possess a noticeable light scattering. The technique for fabrication of nanorings 110 nm in diameter from silver is described in [11]. The same work reports on surface plasmons on these rings as excited by radiation with a wavelength of 1000 nm.

Proceeding from equalities (17) and substituting κ_{0z} from the formula $\kappa_{0z} = \sqrt{k_{0x}^2 - (\omega/c)^2\varepsilon_1\mu_1}$, we can plot two curves $k_{0x} = \varphi_1(\kappa_{2z})$ and $k_{0x} = \varphi_2(\kappa_{2z})$:

$$\begin{aligned} k_{0x} = \varphi_1(\kappa_{2z}) &= \sqrt{\left(\frac{\kappa_{2z}\varepsilon_1}{e_2}\frac{1+e^{-\kappa_{2z}d_2}}{1-e^{-\kappa_{2z}d_2}}\right)^2 + (\omega/c)^2\varepsilon_1\mu_1}\ , \\ k_{0x} = \varphi_1(\kappa_{2z}) &= \sqrt{\left(\frac{\kappa_{2z}\varepsilon_1}{e_2}\frac{1-e^{-\kappa_{2z}d_2}}{1+e^{-\kappa_{2z}d_2}}\right)^2 + (\omega/c)^2\varepsilon_1\mu_1}\ . \end{aligned} \tag{18}$$

At $\kappa_{2z}d_2 \gg 1$ both curves coincide, having the form

$$k_{0x} = \sqrt{(\kappa_{2z}\varepsilon_1/\varepsilon_2)^2 + (\omega/c)^2\varepsilon_1\mu_1}\ . \tag{19}$$

In the theory of surface plasmons, one usually constructs the functions $\omega = \omega(k_{0x})$. Hereafter, we do not consider this dependence and write down all formulas at $\omega = \text{const}$.

At $\kappa_{2z} = 0$, using formulas (18), we obtain

$$\begin{aligned} \min_1 k_{0x} &= \varphi_1^{\min_1}(\kappa_{2z}) = \sqrt{(2\varepsilon_1/d_2e_2)^2 + (\omega/c)^2\varepsilon_1\mu_1}\ , \\ \min_2 k_{0x} &= \varphi_2^{\min_2}(\kappa_{2z}) = (\omega/c)\sqrt{\varepsilon_1\mu_1}\ , \end{aligned} \tag{20}$$

Curves (18) are the geometric locus of pairs of points κ_{2z} and k_{0x} or, respectively, κ_{2z} and κ_{0z}, which turn the denominators in formulas (16) to zero. However, when choosing κ_{2z}, the value of k_{0x} (or vice versa) is obtained from the formula

$$\kappa_{2z} = \sqrt{k_{0x}^2 + (\omega/c)^2 e_2\mu_2}\ . \tag{21}$$

Intersection of curves by formulas (21) and (18) or (19) yields the wave number of the surface plasmon $k_{0x}^{\text{pl}} = (\omega/c)\sqrt{\varepsilon_1\varepsilon_2/(\varepsilon_2+\varepsilon_1)}$.

Figure 6 shows the behavior of curves (18), (19), and (21), where the thickness of the silver layer is 50 nm. Of the three almost vertical curves in Fig. 6, the left-hand side curve belongs to the plasmon with a lower space frequency; the right-hand side curve, to the plasmon with a larger space frequency; in between them, to the plasmon on the surface of the infinitely thick metal. The slopping curve was plotted by formula (21).

Curves (18), (19), and (21) intersect at values of k_{0x} from $1.26 \cdot 10^5$ cm^{-1} up to $1.32 \cdot 10^5$ cm^{-1}, which exceeds $1.221 \cdot 10^5$ cm^{-1}, the value of $k_0 = \omega_0/c$, by not much. Intersections are spatial frequencies of plasmon resonances. Waves with a sufficiently arbitrary spatial frequency k_{0x} can be excited on the surface, including short waves, e.g., with $k_{0x} = 0.9 \cdot 10^6$ cm^{-1}. The inserts show the amplitudes of the excited waves. On two upper inserts, one can see that close to the plasmon resonance the amplitudes of the surface waves exceed the amplitude $H_{0y}(z = d_1)$ of the adjacent wave 10^7 times (left, for the symmetric plasmon and right, for the antisymmetric plasmon); in the absence of the resonance, see the

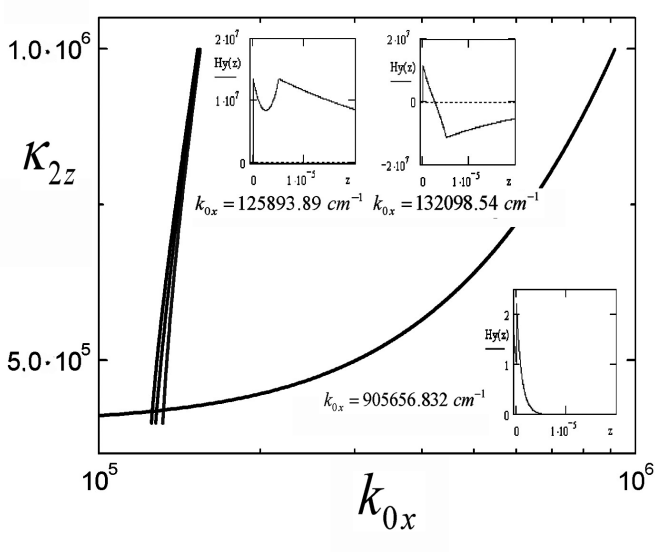

Fig. 6. Behavior of curves (18), (19), and (21) at a thickness of the silver layer of 50 nm.

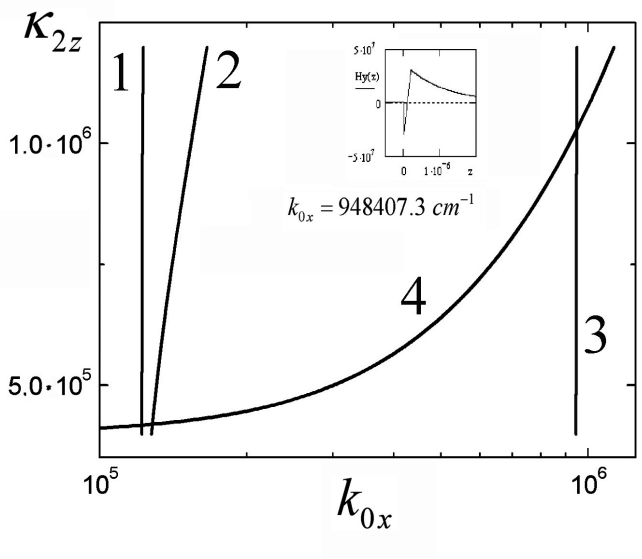

Fig. 7. The same as in Fig. 6 at a thickness of the silver layer of 2 nm.

lower insert, the amplitude is approximately equal to $2H_{0y}(z = d_1)$. Away from the plasmon resonance, the amplitude of the surface wave is small. This poses the problem of increasing the efficiency of excitation of short-wave surface waves.

This problem is solved by changing over to small-thickness metal layers. Figure 7 presents the same curves as in Fig. 6 but for a 2-nm thick silver layer. Of the three almost vertical curves in Fig. 7, the left curve belongs to a plasmon with smaller spatial frequency; the right curve, to a plasmon with a larger spatial frequency; and the curve in between them, to a plasmon on an infinitely thick metal surface. The

gently slopping curve is plotted by formula (21).

Splitting of plasmon modes for this film is significantly increased as compared to splitting for a 50-nm film. Curve (21) in this case intersects with that for the antisymmetric plasmon at $k_{0x} \approx 0.95 \cdot 10^6$ cm^{-1}. On the inset in Fig. 7, one can see that close to this value of k_{0x} the amplitude of the excited wave proves again to be extremely large, exceeding $H_{0y}(z = d_1)$ by more than 10^7 times.

The revealed efficient excitation of short (∼50 nm) surface waves whose wavelength is almost ten times smaller than the wavelength in a vacuum at a chosen frequency, opens a vista for the development of the optics of very short surface waves (i.e., optical transformations such as deviation, focusing, Gaussian beams, photon crystals, etc.). This possibility may prove very useful in applications. Let us calculate the propagation losses of these waves. We will make this calculation in the same way as was made for the plasmon on the surface of an infinitely-thick metal in [7].

We need to find the complex root of the equation

$$\frac{2}{d_2} - \frac{e_2 k_{0x}}{\varepsilon_1}\left[1 - \left(\frac{\omega}{c}\right)^2 \frac{\varepsilon_1 \mu_1}{2k_{0x}^2}\right] = \sqrt{k_{0x}^2 + \left(\frac{\omega}{c}\right)^2 e_2 \mu_2}\,. \tag{22}$$

Then we find $\mathrm{Im} k_{0x}$ at $e_2 = e_2' + ie_s''$.

We shall consider that $e_2 = e_2' + ie_s''$ and that $e_2' \gg e_s''$. Correspondingly, we shall believe that $k_{0x} = k_{0x}' + ik_{0x}''$ and that $|k_{0x}'| \gg |k_{0x}''|$. Let us make conversions in (22):

$$-\frac{e_2}{k}\left[(\delta - \eta)(2k^2 - 1) + 4\eta k^2\right] = \sqrt{k^2 + e_2}\frac{\delta e_2 + 2\eta k^2}{k^2 + e_2}\,. \tag{23}$$

Here, instead of e_2, we take $e_2(1 + i\delta)$ and instead of k_{0x}/k_0, we take $k(1 + i\eta)$; δ and η are small values, and $\varepsilon_1 = \mu_1 = \mu_2 = 1$. As a result, we get

$$k_{0x}'' = -e_2'' k_{0x} \frac{k + (2k^2 - 1)\sqrt{k^2 + e_2}}{2k^3 + e_2(2k^2 + 1)\sqrt{k^2 + e_2}}\,. \tag{24}$$

If we take into account that $k \gg 1$, then we have

$$k_{0x}'' \approx -\frac{e_2''}{e_2} k_{0x}\left(e_2 - \frac{k}{e_2\sqrt{k^2 + e_2}}\right) \approx -\frac{e_2''}{e_2} k_{0x}. \tag{25}$$

At a wavelength of 514.5 nm, the ratio $|\varepsilon'|/\varepsilon''$ is ∼30. This implies that the wave path is about 30 wavelengths. Figure 8 shows that at a wavelength of about 1000 nm the wave path can be up to 100 wavelengths.

Consider in more detail the structures with a metal layer. Using the effect of a metal layer, we can construct a signal coupler from a plane optoelectronic structure or a lightguide. The possibility of greater spatial freedom by using a coupler could be useful in practice. The dispersion of the effect of amplification of the evanescent wave penetrating through a metal layer can be used in a sensitive device for measuring the wavelength in an experiment similar to the experiment with total internal reflection, or for measurements of the size of the structural elements in nanodevices generating evanescent waves in the space adjacent to the nanodevice.

Of (practical) interest is the development of the optics of two-dimensional (2D) surface waves at a dielectric–metal interface, similar to the optics of three-dimensional (3D) waves in 3D space. As in 3D optics, the use of lenses, prisms, mirrors, diffraction gratings, photon crystals, lightguides, etc. is possible

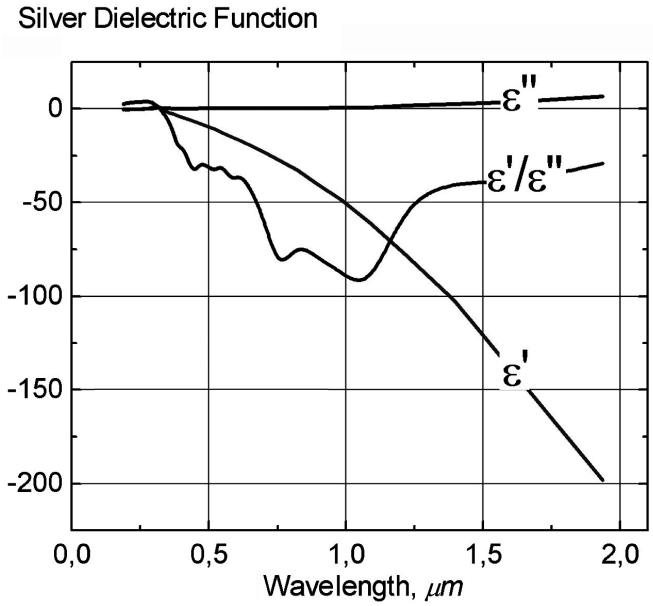

Fig. 8. Permittivity of silver at various wavelengths (according to the data from [9]). The relation $\varepsilon'/\varepsilon''$ is also shown.

here. Two things are an advantage: (i) surface waves occupy a limited plane layer and (ii) surface waves are noticeably slower than waves in 3D space. Optical devices with surface waves can be combined into multilayer (multistack, to be more exact) structures. The structural elements shall be more fine than similar elements in 3D space, as diffraction restrictions will come into play at, respectively, small sizes owing to the smallness of the length of the surface wave. Absorption, peculiar to the surface waves, can be overcome by applying a thin amplifying layer, as demonstrated in [12].

6. Conclusions

The program of the 89th OSA Annual Meeting and Laser Science XXI on the Frontiers in Optics 2005 to be held October 26 (the program is posted on the website of the American Optical Society) includes a report by Prof. Eli Yablonovich, University of California at Los Angeles (USA) on Plasmonics: Optical Frequencies with X-Ray Wavelengths. As judged by the title, this presentation deals with the idea voiced in the above paragraph. It is true, though, that x-ray wavelengths are wavelengths of photons with an energy greater than 1 kV, i.e., wavelengths of 1 nm and shorter. If one has in mind dielectrics, then by the method of total internal reflection optical surface waves of such small length on plane interfaces can be obtained using a dielectric with an unreal value of $\varepsilon\mu = 2.5 \cdot 10^5$. On nanocylinders from a metal, there is an additional deceleration [10], which can be called geometric. The surface wave can be decelerated 30 to 40-fold. A segment of a nanocylinder can serve as a device for exciting the short surface wave.

For a thin layer of metal and, possibly, for the metal surface layer, the values of ε and μ may differ from those for a massive metal layer. The issue requires a separate study.

Surface waves exist not only as plasmons, but also as surface polaritons; see, e.g., [13]. The existence of weakly decaying evanescent waves at the interface between the traditional dielectric and the so-called

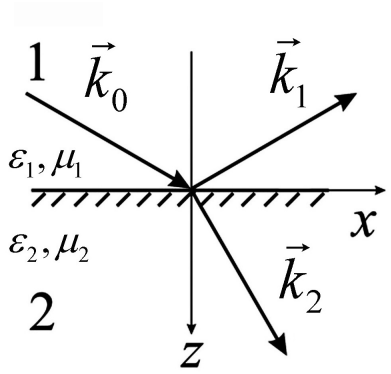

Fig. 9. Designations for an experiment with a plane wave incident on the plane interface between two media with different values of ε and μ.

photon crystal is also predicted [14]. In this paper, we were interested in predicting small propagation losses. The problem requires additional research.

For the completeness it is necessary to mention the paper [15] appeared in 2005 at the moment of accomplishment of the present work. The paper [15] demonstrates a compensation effect for plasmon propagation losses by usage of a thin layer of an excited dye solution that underlays the metal film. The paper [15] has a direct relation to Sec. 5 of this paper because it radically solves the problem of propagation losses.

Acknowledgments

The author is grateful to Professor E. M. Dianov for suggesting the topic and for interest in this work.

Appendix

The table below presents expressions for fields of plane waves at the plane interface between two media with different permittivities and permeabilities, ε_1, μ_1 and ε_2, μ_2, respectively. The dependence on time is chosen as $e^{-i\omega t}$. The formulas refer to the TM wave (the so-called transverse magnetic wave). The x-axis is directed along the surface; the z-axis, normal to the interface surface towards the second medium. The surface $z = 0$ coincides with the plane of the interface. The formulas are applicable for media with $\varepsilon < 0$, $\mu < 0$ and for evanescent plane waves in which the projection k_{2z} is a purely imaginary value. The fields have subscripts, of which 0 pertains to the incident wave; 1, to the reflected wave; and 2, to the refracted wave. These formulas substitute for the usually used formulas with angles of incidence, reflection, and refraction for reflected and refracted waves. In this paper, these angles would have to be replaced by an angular coordinate, which, certainly, is also acceptable.

$H_{0y}(\vec{r}) = H_{0y}e^{i(k_{0x}x+k_{0z}z)}$,	$E_{0x}(\vec{r}) = \frac{ck_{0z}}{\omega\varepsilon_1}H_{0y}e^{ik_{0z}z}e^{ik_{0x}x}$, $E_{0z}(\vec{r}) = -\frac{c\kappa_{0x}}{\omega\varepsilon_1}H_{0y}e^{ik_{0z}z}e^{ik_{0x}x}$,
$H_{1y}(\vec{r}) = \frac{1-K}{1+K}H_{0y}e^{i(k_{0x}x-k_{0z}z)}$,	$E_{1x}(\vec{r}) = -\frac{ck_{0z}}{\omega\varepsilon_1}H_{0y}e^{i(k_{0x}x-k_{0z}z)}$, $E_{1z}(\vec{r}) = -\frac{c\kappa_{0x}}{\omega\varepsilon_1}\frac{1-K}{1+K}H_{0y}e^{i(k_{0x}x-k_{0z}z)}$,
$H_{2y}(\vec{r}) = \frac{2}{1+K}H_{0y}e^{i(k_{2x}x+k_{2z}z)}$,	$E_{2y}(\vec{r}) = \frac{ck_{2z}}{\omega\varepsilon_2}H_{0y}e^{i(k_{2x}x+k_{2z}z)}$, $E_{2z}(\vec{r}) = -\frac{ck_{2x}}{\omega\varepsilon_2}H_{0y}e^{i(k_{2x}x+k_{2z}z)}$.

In the table, $K = k_{2z}\varepsilon_1/k_{0z}\varepsilon_2$ and the following relations between the wave numbers of the waves involved

$$\begin{gathered} k_{0x} = k_{1x} = k_{2x}, \\ k_{0z} = \sqrt{(\omega/c)^2\varepsilon_1\mu_1 - k_{0x}^2}\,, \qquad k_{1z} = -\sqrt{(\omega/c)^2\varepsilon_1\mu_1 - k_{0x}^2} = -k_{0z}, \\ k_{2z} = \sqrt{(\omega/c)^2\varepsilon_2\mu_2 - k_{0x}^2}\,, \quad for \quad k_{0x}^2 \le (\omega/c)^2\varepsilon_2\mu_2, \\ k_{2z} = i\sqrt{(k_{0x}^2 - \omega/c)^2\varepsilon_2\mu_2}\,, \quad for \quad k_{0x}^2 > (\omega/c)^2\varepsilon_2\mu_2, \end{gathered} \tag{A.1}$$

are taken into account.

Relations (1) occur due to the equality of the tangential components of the fields at the interface:

$$\begin{aligned} H_{0y}(\vec{r},t)|_{z=0} + H_{1y}(\vec{r},t)|_{z=0} &= H_{2y}(\vec{r},t)|_{z=0}\,, \\ E_{0x}(\vec{r},t)|_{z=0} + E_{1x}(\vec{r},t)|_{z=0} &= E_{2x}(\vec{r},t)|_{z=0}\,. \end{aligned} \tag{A.2}$$

The sign of k_{0z} is taken arbitrarily positive. For k_{1z}, the sign is taken to be opposite to that of k_{0z}, since otherwise we would have an incident wave. For k_{2z} we choose the plus sign so that the wave moves away from the surface.

References

1. V. G. Veselago, *Uspekhi Fiz. Nauk*, **92**, 517 (1967) [*Sov. Phys. – Uspekhi*, **10**, 509 (1968)].
2. D. R. Smith, W. J. Padilla, D. C. Vier, et al., *Phys. Rev. Lett.*, **84**, 4184 (2000).
3. J. B. Pendry, *Phys. Rev. Lett.*, **85**, 3966 (2000).
4. X. S. Rao and C. K. Ong, arXiv:cond-mat/0304133, v2, June 16, 2003.
5. X. S. Rao and C. K. Ong, arXiv:cond-mat/0304474, v2, July 2, 2003.
6. M. Born and E. Wolf, *Principles of Optics*, Pergamon Press, Oxford (1983).
7. H. Raether, *Surface Plasmons*, Springer-Verlag, Berlin (1988).
8. G. J. Kovacs and G. D. Scott, *Phys. Rev.* B, **16**, 1297 (1977).
9. P. B. Johnson and R. W. Christy, *Phys. Rev.* B, **6**, 4370 (1972).
10. V. S. Zuev, G. Ya. Zueva, and A. V. Frantsesson, *Opt. Spektrosk.*, **95**, 394 (2003).
11. J. Aizpurua, P. Hanarp, D. S. Sutherland, et al., *Phys. Rev. Lett.*, **90**, 057401 (2003).
12. J. Seidel, S. Grafström, and L. Eng, *Phys. Rev. Lett.*, **94**, 177401 (2005).
13. H. Failache, S. Saltiel, A. Fisher, et al., *Phys. Rev. Lett.*, **88**, 243603 (2002).
14. D. Artigas and L. Torner, *Phys. Rev. Lett.*, **94**, 013901 (2005).
15. J. Seidel, S. Grafstroem, and L. Eng, *Phys. Rev. Lett.*, **94**, 177401 (2005).